Fuel 358 (2024) 130254

Contents lists available at ScienceDirect

Fuel

journal homepage: www.elsevier.com/locate/fuel

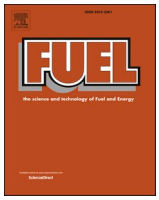

Full Length Article

Formation, coalescence and behaviour of bulk nanobubbles in dodecane and isooctane and their thermophysical properties: A comprehensive molecular study

Hamidreza Hassanloo *, Xinyan Wang

Centre for Advanced Powertrain and Fuels, Brunel University London, Uxbridge UB8 3PH, United Kingdom

ARTICLE INFO

Keywords:
Phase change material
Nanobubbles
Isooctane
Thermal properties
Nucleation and coalescence
Molecular dynamics simulations

ABSTRACT

In recent decades, nanobubbles (NBs) have attracted great attentions of researchers in a number of fields, including aquaculture, water treatment, biomedical engineering and energy/power engineering. However, the fundamental understanding of these tiny bubbles through experimental techniques is very challenging. Dodecane, as a phase change material with a high boiling point, and isooctane, as an alternative fuel with high octane number and low volatility, have been researched and used in energy applications. In this work, the nucleation, coalescence and behaviour of formed NBs of carbon dioxide (CO_2), oxygen (O_2), nitrogen (N_2), and hydrogen (H_2) gases in dodecane and isooctane samples as well as their effects on the thermo-physical properties of the samples were investigated by means of molecular dynamics (MD) simulations. The weight fraction of the added gas and temperature were also investigated to understand their effects on the bubble dynamics and inherent properties. The results reveal that the addition of CO_2 gas leads to the biggest drop in the viscosity of the dodecane by 20.47%, while the dispersion of oxygen gas in dodecane increases the viscosity. It is also found that samples containing NBs have higher specific heat capacity than samples without NBs and the highest specific heat capacity improvement can be obtained by dissolving hydrogen NBs. Furthermore, it is found that specific heat capacity of isooctane sample increases by increasing the weight fraction of dispersed gas. However, dodecane shows the opposite trend. By increasing the system temperature, the specific heat capacity of dodecane sample increases while isooctane sample again shows the opposite trend.

1. Introduction

Nanobubbles (NBs), tiny bubbles with dimeter less than 1000 nm, have emerged as a promising solution to a wide range of technological challenges [1]. One of the areas where NBs have shown potential is in the use of phase change materials (PCMs), used for latent heat energy storage (LHTES) in order to decrease the dependence of renewable energy on secondary energy sources [2–4], and fuel processing to improve energy conversion efficiency and reduce emissions of combustion engines [5]. Specifically, the unique properties of NBs, for example high surface area, can enhance the thermal properties of PCMs which are useful in applications where rapid heat transfer is important, such as in solar energy storage [6,7]. It was found that blending NBs with conventional fuel like gasoline causes a decrease in the emission of harmful gases by reducing the brake specific fuel consumption (BSFC) due to the improved fuel atomization and combustion process with the added nanobubbles [5].

Phenomena and materials show abnormal behaviour at nanoscale and do not obey the accepted theories at this scale. For instance, unlike the prediction of Epstein-Plesset theory, NBs can exist in host liquids for a long period [1,8,9]. This unique behaviour provides possibilities of producing engineered materials with desirable properties via nanotechnologies for different applications [10,11]. However, due to the limitation of experimental techniques, study and characterisation of the behaviour at nanoscale is very challenging. Instead, molecular approaches like molecular dynamic (MD), Monte Carlo (MC), and coarse-grained (CG) simulations are widely used to investigate nanoscale phenomena that could affect the bulk behavior and properties of generated materials [12–16]. NB is one of these new phenomena that attracts great attentions of researchers in recent years. Experimental and numerical studies have been conducted to investigate these nebulous tiny bubbles with unique properties.

* Corresponding author.
E-mail address: Hamidreza.Hassanloo@brunel.ac.uk (H. Hassanloo).

https://doi.org/10.1016/j.fuel.2023.130254
Received 24 August 2023; Received in revised form 11 October 2023; Accepted 29 October 2023
Available online 3 November 2023

An experimental study by Sinah-Ray et al. [17] reveals that adding surfactants to an oil-based heat transfer fluid as a coolant for a micro-channels gives a rise to formation of air bubbles. These NBs improve heat transfer by increasing the flow rate. It was found that the existence of CO_2 NBs in food fluids can affect their thermophysical properties [18]. The viscosity of the treated liquids has direct relationship with the concentration of dissolved gas as the lowest viscosity was reported for the liquid with highest concentration of the dissolved gas [18]. As inherent properties of materials play an important role in their applications, researchers have tried to use molecular approaches to investigate these properties. The nucleation of 240 dissolved gas atoms in liquid medium with 5839 atoms in nanochannels with hydrophobic and hydrophilic surfaces was studied by using molecular dynamics simulations [19]. It was found that the coalescence occurs right after the nucleation, which leads to the growth of NBs and movement toward the surfaces. These large bubbles replace the liquid layer and cause the drag reduction [19]. Generation of vapor NBs in the existence of heated nanoparticles and dissolved gas was investigated by using numerical methods by Maheshwari et al [20]. It was reported that the critical temperature of host liquid decreases due to the existence of dissolved gas which improves the nucleation process. Wang et al. [21] studied the thermodynamic properties of crystalline octadecane and octadecane-water slurry by using condensed-phase optimized molecular potentials for atomistic simulation studies (COMPASS) force field. Thirteen octadecane molecules chains resulting in 840 atoms in total were used to create nano-capsule with radius 24.4 $\dot{A}$. Then the prepared nano-capsule was placed in three different water simulation boxes including 1470, 2083 and 3309 water molecules, respectively. It has been found that the heat capacity of octadecane slurry decreases with the increase of octadecane mass fraction. The diffusion coefficient of binary mixtures of carbon dioxide with methanol was investigated by Chatzis and Samios [22]. They used the OPLS, EPM2 models and the Lorentz–Berthelot combining rules to simulate the interaction between molecules. They observed that the diffusivities of species decrease with the increase in pressure. Five types of gases, namely H_2, CH_4, CO, O_2, and CO_2, were dissolved in water to study the effects of type of dissolved gas on the transport properties of the polar host. In this numerical study by using molecular approaches, it was found that the diffusion coefficient of the prepared samples highly depends on the type of the dissolved gas [23].In an experimental study, the role of dissolved krypton, N_2 and O_2 gases on the nucleation and stability of bulk NBs in water were investigated. Results illustrate that the concentration of NBs depend on the type of scattered gas [24]. It was also reported that the nucleation of bulk NBs highly depend on the concentration of the dissolved gas. The dimeter of the generated NBs in water is increased by increasing the weight fraction of dissolved gas [25]. In addition, it was observed that by decreasing temperature, the possibility of NBs formation decreases, which illustrates the role of temperature in the generation of bulk NBs [26].

Dodecane has a relatively high boiling point of 215 °C, which makes it useful in high-temperature applications, such as heat transfer fluids in solar thermal power plants or industrial processes as PCM. Phase change temperature of dodecane makes it as one of the potential candidates for cold chain transportation application. Inherent properties of dodecane also make it as a useful lubricant or fuel. In addition, its biodegradability makes it a more environmentally friendly alternative to other hydrocarbon solvents [27–30]. In comparison, a high-octane rating of isooctane results in cleaner and more efficient combustion process in power systems than other lower-octane hydrocarbon fuels like gasoline and diesel. Isooctane has low volatility and its resistance against engine knock and its capacity in blending with renewable fuels makes its one of the alternative fuels to reduce harmful emissions from internal combustion engines [31]. Inherent properties of these two potential liquids for renewable applications have been researched and improved by adding or blending various materials to them in order to prepare them for industrial applications [32,33]. Nanobubbles are an active research field in various areas of science and engineering and primary studies reveal its potential in power and energy systems [34,35]. In this study, for the first time, the formation, behaviour, and effects of bulk NBs on thermophysical properties of dodecane and isooctane were investigated by using MD simulations. The impacts of gas type, weight fraction of dissolved gas and system temperature were also investigated and analysed.

Table 1
The comparison of inherent properties calculated by MD simulation and experimental values at 25 °Celsius and 1 atmosphere [49–51].

Liquids	Number of atoms	Potential	Density (kg/m^3)	Viscosity (Pa.s)	Diffusion Coefficient (m^2/s)
Dodecane	190,000	Compass	0.73876	0.00127	1.06×10^{-9}
		Experimental	0.746	0.00134	0.871×10^{-9}
Isooctane	166,400	Compass	0.678	0.000375	2.59×10^{-9}
		Experimental	0.687	0.000474	–

2. Theory and modelling

Computational nanoscience serves as an indispensable research tool, facilitating the modeling, comprehension, and prediction of nanoscale phenomena. It employs various methods, including classical molecular dynamics, density functional approaches, and fully correlated wave functions, to solve physical problems at different levels of sophistication. In quantum mechanics (QM), the Schrödinger equation is solved to elucidate molecular interactions, potential energy surfaces, and charge distributions. Among QM-based techniques, ab initio molecular dynamics (AIMD) stands out, rooted in density functional theory (DFT) and prominently Car–Parrinello molecular dynamics (CPMD). AIMD combines classical nuclear dynamics with quantum electron dynamics, providing a powerful approach for simulating complex systems, albeit with smaller accessible correlation lengths and relaxation times compared to classical molecular dynamics. While AIMD offers a deeper understanding of quantum behaviors, it demands substantial computational resources, limiting its performance, especially in simulating multicomponent liquids [36–39]. In contrast, classical molecular dynamics, treating atoms and bonds as a balls-and-springs and using Newtown's second law and different potentials to calculate the atomic interactions and predict the motions of atoms enables researchers to study the complex system from molecular approaches. In the first place, molecular topology and interaction potential are defined. Then initial positions, velocities, and simulation conditions like temperature and pressure are defined. By using the selected potentials and the equation of motion, tangible parameters like per-atom energies (potential and kinetic) are calculated to use directly or in other methods like Green-Kubo to clarify the atomic mechanism behind the bulk behavior of materials and their thermophysical properties[40,41].

As discussed above, the interactions between atoms which originate from the selected potentials play an important role in the accuracy of this approach. The condensed-phase optimized molecular potentials for atomistic simulation studies (COMPASS) force field was used to describe the interactions between the liquids' atoms[42]. To make sure the selected potential can accurately capture the force between atoms, density, viscosity, and diffusion coefficient of the desired host liquids were calculated. The results show good agreement with experimental measurements, as shown in Table 1. Lenard-Jones potential was used to capture the behavior of gas atoms[43–46]. Detailed information regarding the sample preparation process can be found in the supplementary file's preparation section. All the simulations were carried out by the open-source package of LAMMPS[47]. Ovito software was utilized for the visualization [48].

All the prepared samples were relaxed for 1.7 ns in NPT ensemble

Table 2
Presents the structural features of the prepared samples. more details about the initial structures are provided in the supplementary file.

Sample	Number of molecules		Sample	Number of molecules	
	Gas	Host liquid		Gas	Host liquid
Nitrogen/ Dodecane	1941	5000	Nitrogen/ Isooctane	1640	6300
Oxygen/Dodecane	1699	5000	Oxygen/Isooctane	1436	6300
Carbon dioxide/ Dodecane	2150	8000	Carbon dioxide/ Isooctane	1988	12,000
Hydrogen/ Dodecane	1948	5000	Hydrogen/ Isooctane	1646	6300

and 1.7 ns in NVT ensemble in order to reach an equilibrium under desirable conditions. The simulations were continued for 10 ns in NVE ensemble to investigate the behaviour of NBs and thermo-physical properties of treated dodecane and isooctane. Further details on the the simulation procedure can be found in the Simulation Procedure section of the supplementary file.

In this study, four gases, namely nitrogen, oxygen, hydrogen, and carbon dioxide, were dispersed in the liquid hosts to study the effect of gas types on the formation, coalescence and the behavior of NBs. Besides, the effect of the weight fraction of dissolved gas and system temperature on the bubble dynamics and inherent properties were also studied.

3. Results and discussion

3.1. Impact of host liquids and gas types

Three gases, namely nitrogen, oxygen, and carbon dioxide with the same weight friction (6 wt%) were dispersed in the dodecane and isooctane hosts. Due to the small atomic mass of hydrogen molecule, a different weight fraction was investigated for hydrogen sample. Table 2 and Fig. 1 illustrate the constructional parameters and initial structure of prepared samples, respectively. All the obtained samples were studied under the environmental condition (1 atm and 25 °C).

As shown in Figs. 2 and 3, it was observed that within 13.4 ns, nitrogen, oxygen, and hydrogen can form NBs in the dodecane host, while nitrogen and hydrogen can generate NBs in isooctane host. However,

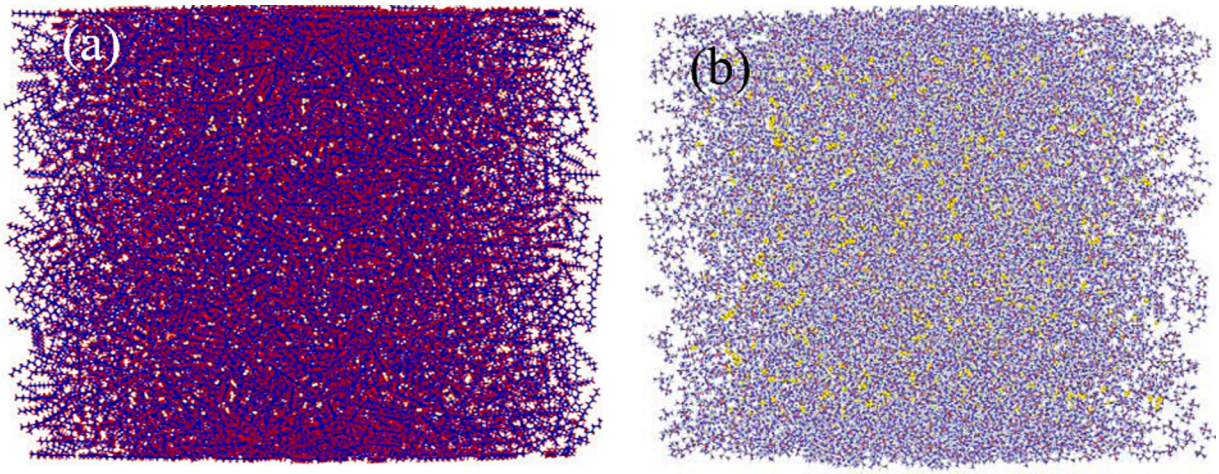

Fig. 1. Initial configuration of the scattered gas in the (a) dodecane and (b) isooctane samples.

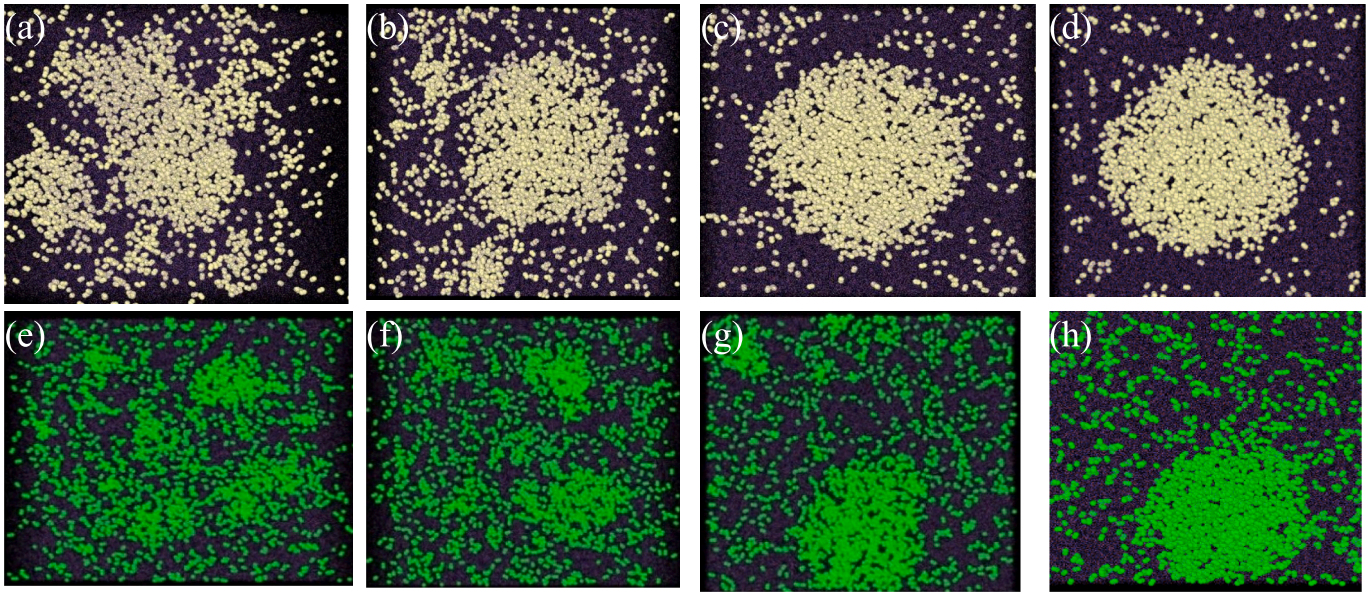

Fig. 2. Formation process of (a, b, c, d) nitrogen and (e, f, g, h) oxygen NBs in PCM host after 1, 1.5, 4.75, and 10 ns (from left to right).

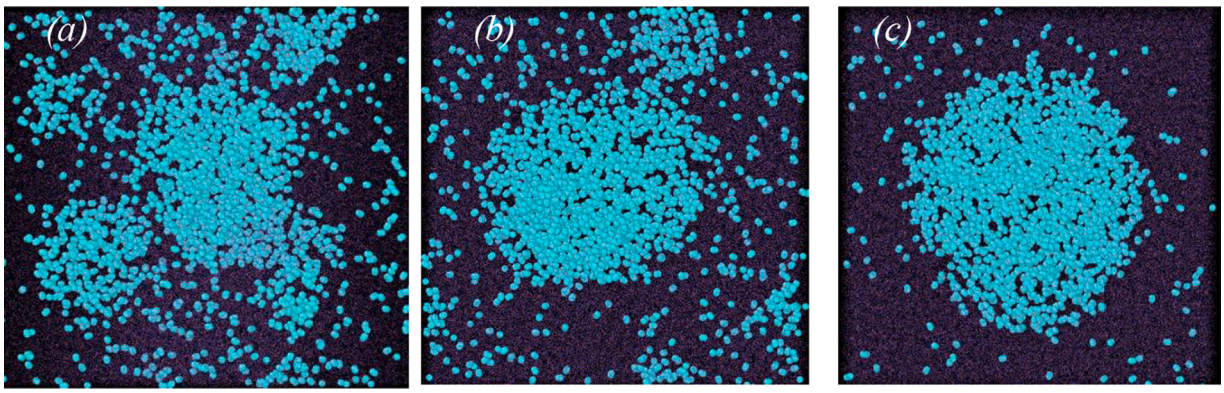

Fig. 3. Formed hydrogen NBs in dodecane at (a) 0.5, (b) 1, and (c) 10 ns.

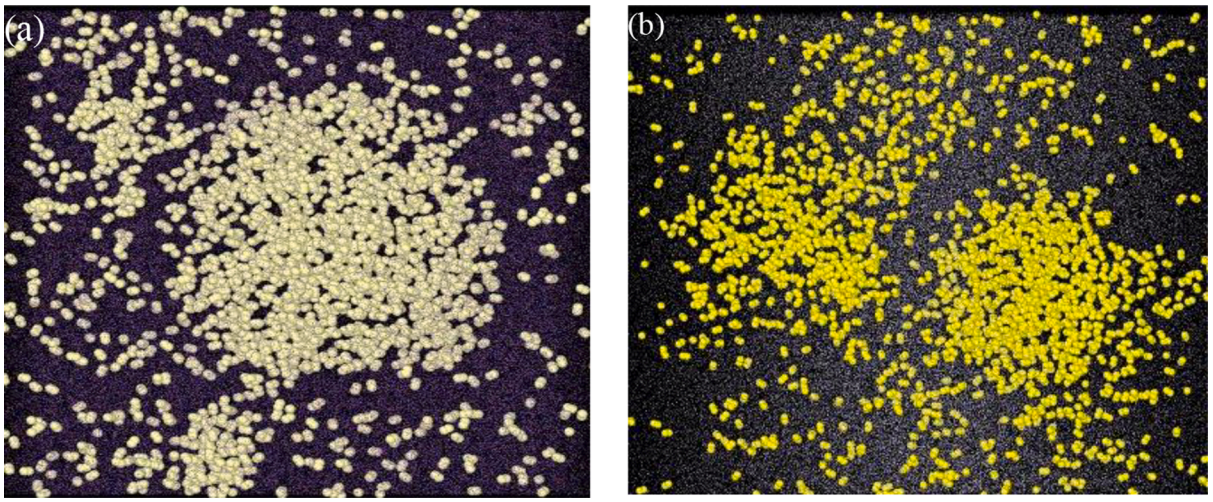

Fig. 4. Formed nitrogen NBs in (a) dodecane and (b) isooctane samples at 1.5 ns.

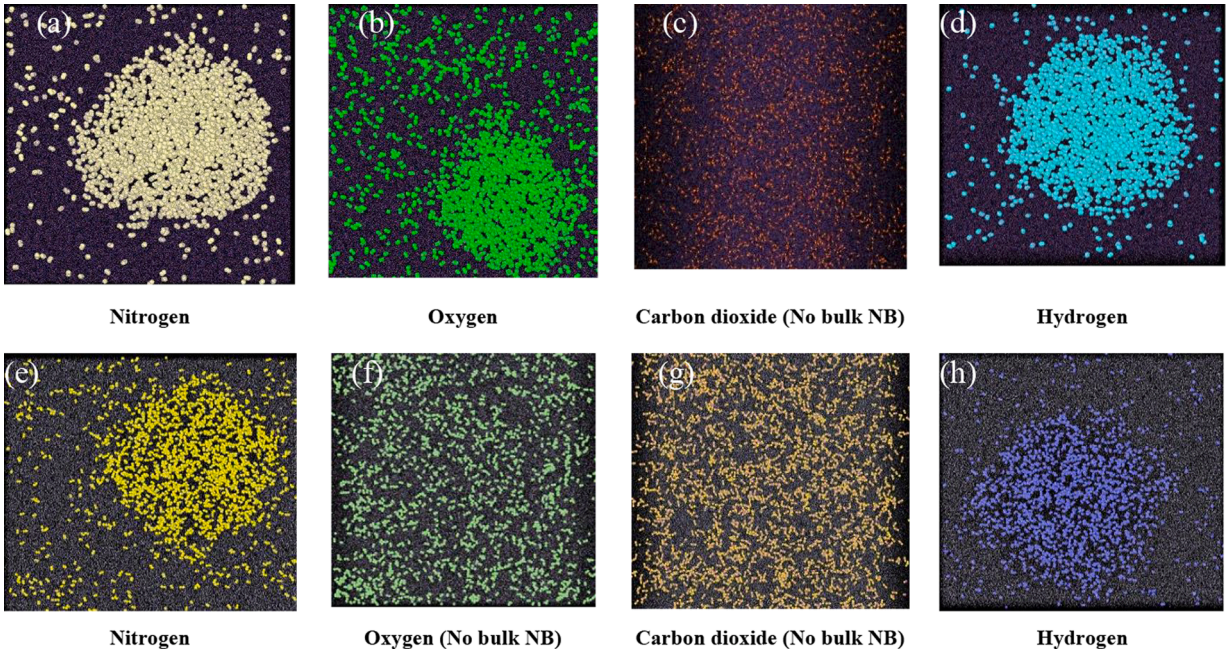

Fig. 5. The NBs formed in (a, b, c, d) dodecane and (e, f, g, h) isooctane samples with different gases at the end of simulation.

Table 3
The viscosity of dodecane and isooctane based samples (Pa.s) with various dissolved gas.

Host liquids	CO_2	N_2	O_2	H_2
Dodecane	0.00101	0.00103	0.00153	0.00113
Isooctane	0.000541	0.00049	0.000445	0.000487

carbon dioxide could not create any NBs in both liquid hosts. Once the initial nucleation sites appear in the host liquids, small NBs start to coalesce to form a larger bubble due to Ostwald ripening. In an experimental study, it was observed that huge amount of dissolved nitrogen molecules can form NBs in the host liquid and majority of the dispersed gas exists in the form of NBs and nearly there were not any homogenous forms of it in the surrounded medium [52].

The comparison of the results at 1, 1.5, and 4.75 ns in Figs. 2 and 3 also suggests that the dynamics of bubble formation and coalescence are affected by the properties of the dispersed gases. It is clear in Fig. 2 that considerable nitrogen gas atoms start to agglomerate and form a big NB with 4 child NBs in the host liquid at 1 ns. It can be observed that the child NBs start to join the mother NB and this process takes about 0.5 ns. However, the oxygen atoms only start to create small NBs at 1.5 ns. Unlike the oxygen atoms, majority of nitrogen atoms exist in the form of bulk NB in the dodecane after 4.75 ns. Therefore, for the same amount of scattered gas, the speed of coalescence process of nitrogen atoms in dodecane sample is higher than that of oxygen atoms. The behavior of scattered hydrogen in Fig. 3 indicates that the bubble dynamics is very dependent on the type of dispersed gas. It can be observed that at 1 ns the majority of the scattered hydrogen atoms already generate a tangible NB in dodecane sample. So, it can be concluded the speed of the formation and coalescence of nanobubbles depends on the type of gas atoms and their molecular interactions.

It is found that at 1.5 ns the majority amount of nitrogen atoms in dodecane exist in a large NB. However, for the same weight fraction of this type of atoms, small NBs in isooctane can be observed at 1.5 ns, as shown in Fig. 4. The most interesting observation is that oxygen atoms could not form any NBs in the isooctane sample, while a large oxygen NB can be observed in dodecane at the end of simulation, as shown in Fig. 5. Therefore, the formation of NBs is also affected by the properties of host liquids. Further examination of the oxygen interaction with dodecane and isooctane, as illustrated in Supplementary Fig. 3, highlights the inhibiting effect of stronger attractive forces between oxygen and isooctane molecules, preventing oxygen molecules from clustering together in the isooctane sample, in contrast to dodecane.

As the transport properties play an important role in the industrial applications of working liquids, the effect of the scattered gas and NBs on the viscosity, specific heat capacity, and diffusion coefficient of the obtained samples were studied after investigating the dynamics of NBs in order to understand the potential of NBs for industrial applications.

Viscosity shows the resistance of materials against the flow and can affect the efficiency of heat transfer as well as the energy consumption of the designed system. Green-Kubo method, as outlined in Supplementary equation (2), was used to calculate the viscosity of the prepared samples.

Table 3 shows the viscosity of the obtained samples. It can be seen that the viscosity of prepared samples decreases by dissolving carbon dioxide, nitrogen, and hydrogen gases, compared to the pure dodecane (Table 1). However, scattering oxygen atoms in dodecane causes an increase in the viscosity, compared to the pure dodecane. The biggest drop in the viscosity of the dodecane sample is caused by the addition of CO_2 gas, which reduces the viscosity by 20.47% compared to pure dodecane.

Fig. 6 compares the Coulomb energy of the dodecane samples with dissolved carbon dioxide and nitrogen. The result reveals that Coulomb energy of CO_2/dodecane sample is higher than the nitrogen one with the same weight fraction. It indicates that repulsive force in the CO_2/dodecane sample prevents the scattered CO_2 to agglomerate in the dodecane host. In addition, due to high repulsive forces in the carbon dioxide sample, atoms can move freely than nitrogen sample, which causes the viscosity of the obtained CO_2 sample to be lower than the nitrogen one. The interaction between dodecane and the dissolved oxygen and nitrogen is captured in Fig. 6b. It is noted that adding oxygen gas increases the attractive force, which leads to the increase in viscosity. Therefore, with the same specific weight fraction, the viscosity of the O_2/dodecane sample is higher than the N_2 one. In the final segment of the simulation procedure outlined in the supplementary file, a detailed description of the energy calculation method employed in this paper was provided.

As discussed in Fig. 5, both nitrogen and oxygen can form NB in dodecane sample. Comparison of the size of the generated NB at 13.4 ns demonstrates that although the dimeter of the nitrogen NB, 8 nm, is bigger than the oxygen one, 7 nm, the viscosity of the dodecane containing oxygen gas, as Table 3 shows, is more affected. This indicates that the effect of gas types on the viscosity of the prepared samples is greater than the size of the generated NB. The comparison of the viscosity of hydrogen/dodecane sample with nitrogen one, from Table 3, shows that the effect of gas type on the viscosity of the prepared samples is greater than the effect of weight fraction, as the viscosity of hydrogen/dodecane sample with smaller weight fraction of scattered gas is higher

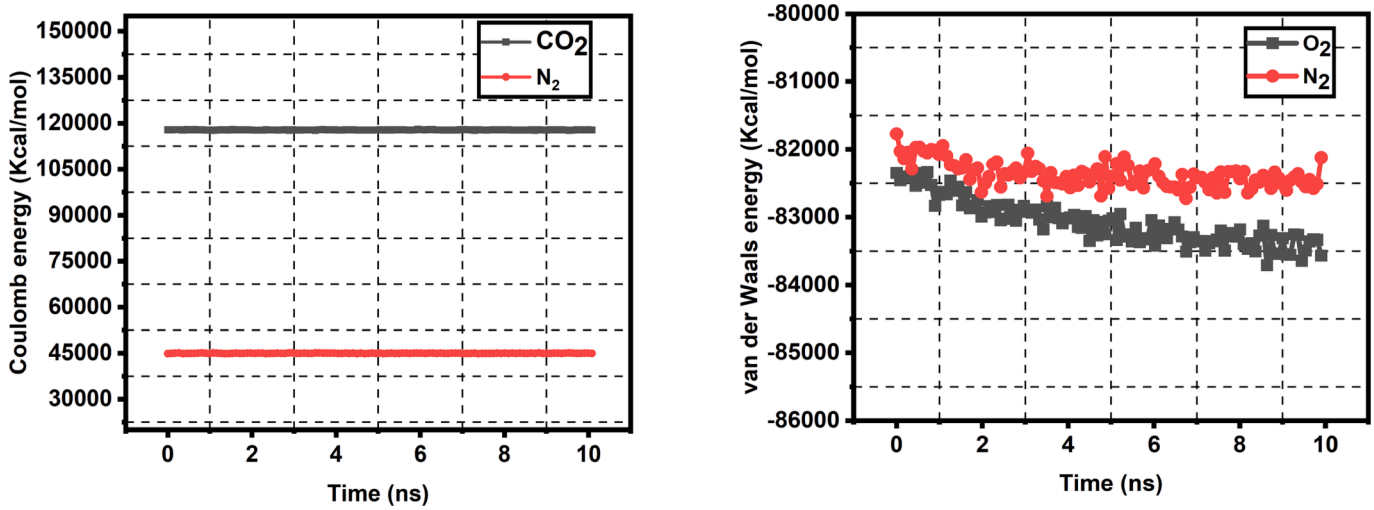

Fig. 6. (a) Coulomb energy of the carbon dioxide and nitrogen system. (b) Van der Waals energy of nitrogen and oxygen samples. Note that the negative sign shows the attractive force and the absolute amount of it should be used for comparing.

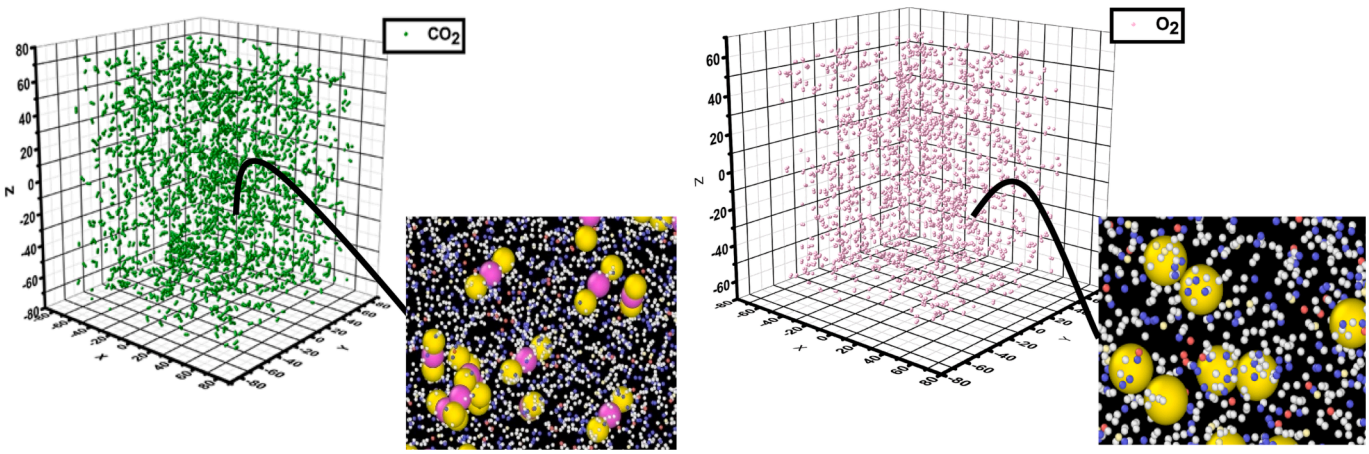

Fig. 7. Distribution of carbon dioxide and oxygen molecular in isooctane-based fluid at the 13.4 ns.

Table 4
The mutual diffusion coefficient of dodecane and isooctane based samples with various dissolved gas (m^2/s).

Host liquids	CO_2	N_2	O_2	H_2
Dodecane	1.24	0.772	0.808	0.8438
Isooctane	2.034	2.055	2.1531	2.4712

than the nitrogen one with higher gas weight fraction.

Unlike the dodecane, the viscosity of isooctane increases when adding carbon dioxide, nitrogen, and hydrogen gases, as shown in Table 3. More specifically, the addition of carbon dioxide produces the highest viscosity, while the addition of oxygen leads to the lowest viscosity of the isooctane mixture. As it was discussed, carbon dioxide and oxygen could not form NB in the isooctane host, however investigating the distribution of CO_2 atoms in isooctane at the end of the simulation time, which is shown in Fig. 7, indicates that carbon dioxide atoms form clusters containing a small number of atoms, for example a cluster with three carbon dioxide atoms, inside the host liquid. Since the number of atoms in these clusters is very small, they cannot be considered as nanobubbles, but their presence affects the movement of atoms, which can act like the scattered obstacles in the path of movement of atoms that reduce their freedom of movement and increases the viscosity of the CO_2/isooctane sample.

The comparison of the van der Waals energy of oxygen and nitrogen isooctane samples confirms that the attractive force in nitrogen mixture causes a strength attraction which decreases the freedom of atoms of this sample and increases the viscosity compared to the oxygen one. The comparison the obtained results of two different host liquids illustrates that the atomic interaction of host liquids and scattered gases has significant effect on the viscosity of the prepared samples. Therefore, molecular interactions should be carefully investigated in order to find the most suitable mixture for a specific energy application.

Fick's law, as described in Supplementary equations 4 and 5, is utilized to calculate the translation motion of molecules within another material, which is known as a diffusion coefficient [15]. Therefore, diffusion coefficient can be used as a measurement of the motion capacity of atoms that can illustrate the structural change of the studied case. Table 4 shows the diffusion coefficient of the prepared samples. As it can be seen that the highest rate of atoms' migration is observed for the sample with lowest viscosity. The comparison of the diffusion coefficient of dodecane samples with oxygen and nitrogen gases, reveals that for the same weight fraction of the scattered gas, the diffusion coefficient of nitrogen sample with larger NB is lower than oxygen one. That means, the diffusion coefficient trends to be lower with larger NB generated in the sample.

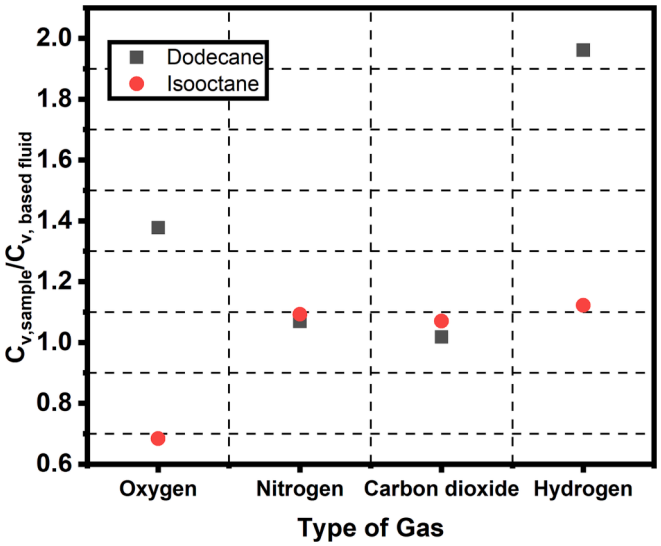

Fig. 8. Specific heat capacity of samples compared to the host mediums.

To measure the heat storage capacity, specific heat capacity at constant volume was calculated by using the following relationship[53]:

$$C_v = \frac{\langle \delta E^2 \rangle}{K_B T^2} = \frac{\langle E^2 \rangle - \langle E \rangle^2}{K_B T^2} \quad (1)$$

in which $\langle E^2 \rangle - \langle E \rangle^2$ is the fluctuation of energy, K_B is Boltzmann constant and T is the temperature. It should be noted that the heat capacity is defined as the required energy to increase the temperature of the system by 1 K. Therefore, it can be considered as the indicator of the stored energy in the system. The comparison of the specific heat capacity of the prepared samples indicates that the addition of nitrogen, oxygen, carbon dioxide, and hydrogen to the dodecane and isooctane leads to an increase in specific heat capacity of host liquids, except the oxygen/isooctane sample (Fig. 8). In addition, it can be observed that the addition of hydrogen in dodecane leads to highest increase of specific heat capacity while carbon dioxide results in least increase. It is found that the addition of hydrogen, carbon dioxide, and nitrogen only leads to a slight increase of specific heat capacity with Cv,sample/Cv,base isooctane liquid around 1.1. More importantly, it is noted that the addition of oxygen in isooctane decreases specific heat capacity. Therefore, the change in specific heat capacity depends on not only the host liquid but also the scattered gas. More investigating the behavior of samples at nano-scale and the effects of NBs formation on the specific isochoric heat capacity reveals that samples containing NBs have higher

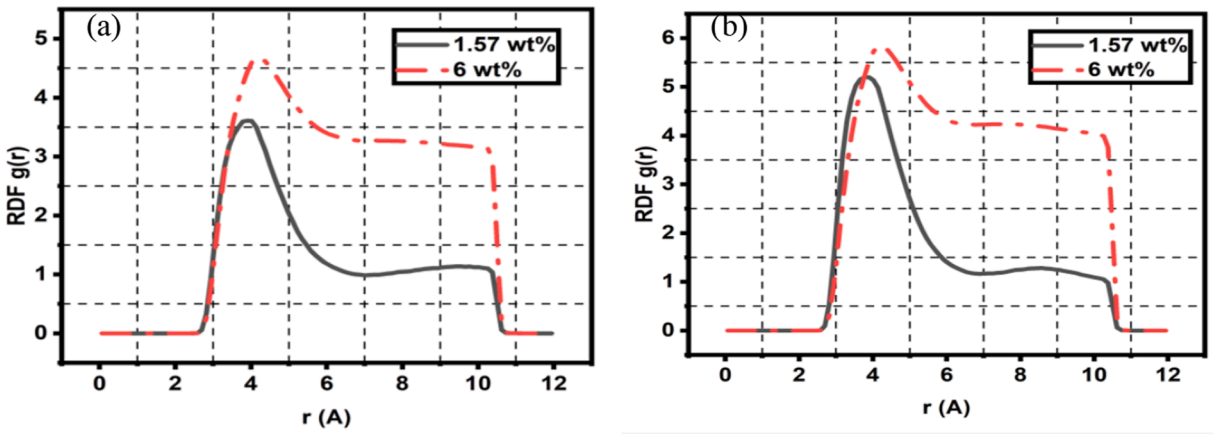

Fig. 9. The radial distribution function (RDF) *of (a) nitrogen gas in isooctane and (b) dodecane samples.*

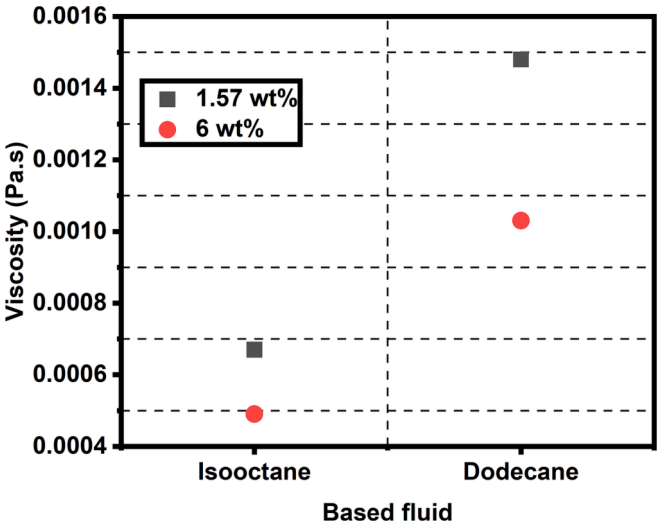

Fig. 10. Viscosity of obtained samples with different gas weight fractions and host liquids.

specific heat capacity than samples without NBs, like oxygen/isooctane sample. The reason of this behavior can be investigated in molecular interactions. Since in samples with stronger attractive forces that lead to the formation of NBs bring about intense collision between atoms that cause increase in thermal properties and specific isochoric heat capacity of bubbled samples [54].

3.2. Effect of gas content

In order to study the effects of concentration of the dissolved gas on the formation mechanism and transport properties, 485 and 410 nitrogen molecules were dissolved in the dodecane and isooctane hosts, respectively, to obtain samples with gas weight fraction of 1.57. Unlike the samples with higher gas weight fraction, as shown in the previous sections, no bulk nanobubbles can be observed in 13.4 ns.

Radial distribution function (RDF) which shows the probability of the existence of atoms in distance r around the specific atoms, can be calculated by using the following equation[55].

$$x_{\upsilon}x_{\xi}\rho g_{\upsilon\xi}(r) = \frac{1}{N}\langle\sum_{i=1}^{N_{\upsilon}}\sum_{i=1}^{N_{\xi}}\delta(r + r_i - r_j)\rangle \quad (2)$$

where x, ρ, $g(r)$, N ,υ, and ξ are mole fraction, density, RDF, the number of total atoms, and the types of chemicals, respectively. The RDFs for gas–gas interactions in samples with varying concentrations of dissolved gas are depicted in Fig. 9. Within Fig. 9, a notable trend emerges in the RDF concerning different gas weight fractions. In cases with higher gas weight fractions, a distinct RDF peak is evident, indicating the presence of a considerable number of gas atoms in close proximity, likely forming gas clusters. Following this peak, a gradual decline in the RDF is observed, implying an increased availability of gas atoms for potential

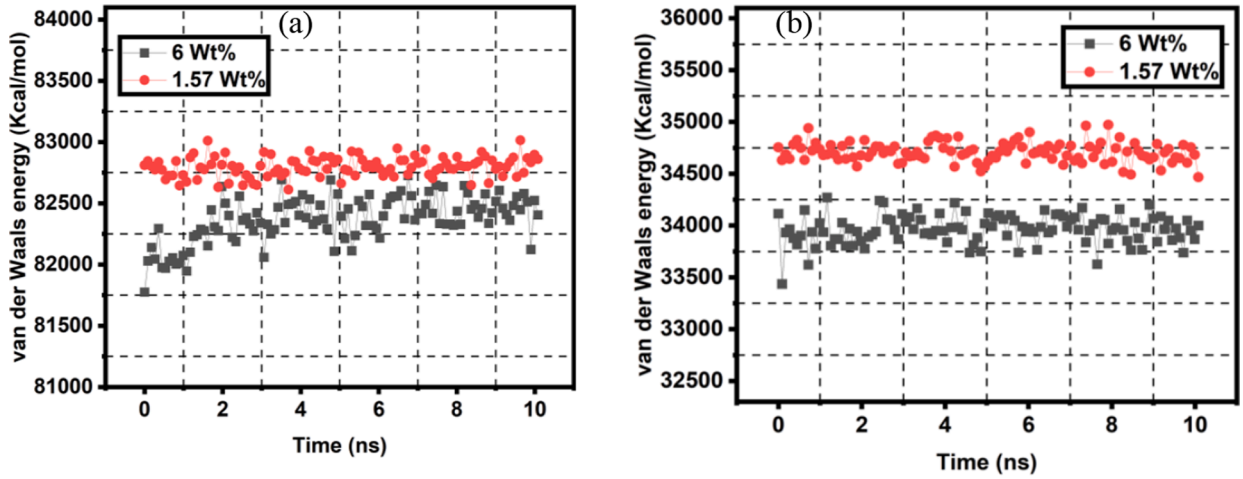

Fig. 11. Absolute amount of attractive energy of samples with various content of scattered gas in (a) dodecane and (b) isooctane.

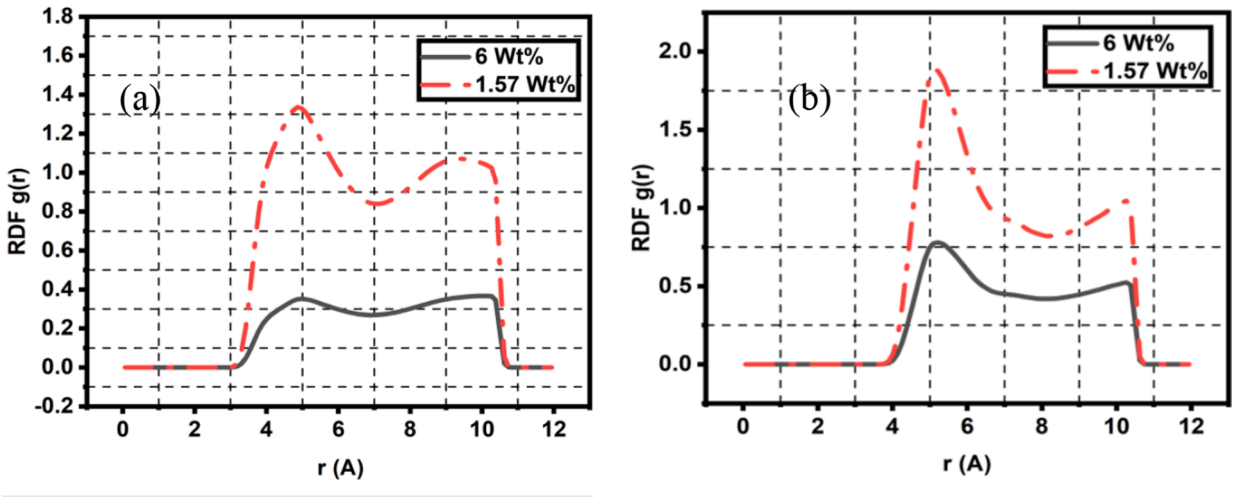

Fig. 12. The radial distribution function (RDF) for the gas-liquid interactions of the prepared (a) dodecane and (b) isooctane samples with different nitrogen concentration.

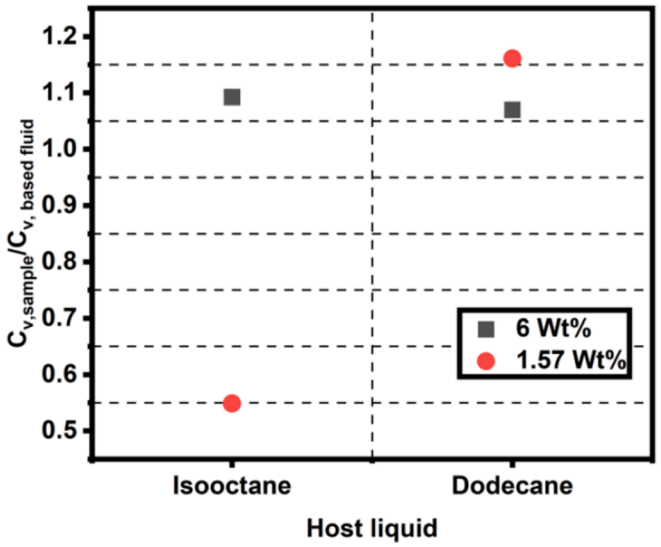

Fig. 13. Comparison of specific heat capacity of mixtures with different gas weight fraction.

NB formation. Conversely, lower gas weight fractions result in a less pronounced RDF peak, suggesting a diminished number of gas atoms in close proximity. Moreover, a significant drop in the RDF is noticeable, signifying an insufficient quantity of gas atoms surrounding the cluster to facilitate NB formation.

It was reported that the viscosity of carbon-based liquids is affected by the dissolved gas in such a way that increasing its concentration reduces the viscosity of the fluids[56]. As shown in Fig. 10, by increasing the concentration of the dissolved gas, the viscosity of the prepared samples decreases.

Fig. 11 shows the van der Waals energy of the obtained samples with different gas weight fraction. As shown in the figure, the van der Waals energy decreases with the increase of gas weight fraction in both liquids. The reduced attractive force between atoms lowers the resistance of samples against flow, which decreases the viscosity of the prepared samples.

Fig. 12 shows the RDF for liquid–gas. The results indicate that the increased gas weight fraction reduces significantly the RDF. Therefore, the number of gas atoms around the liquid atoms decreases with the increase of gas weight fraction, and they can move more freely, leading to increased diffusion coefficient. It was observed that the diffusion coefficient of the prepared samples is increased by 12.91 % and 1.45 % for isooctane and dodecane samples, respectively, when the gas weight fraction increased from 1.57 to 6 wt%, Table 4 shows the diffusion coefficient of 6 wt% of nitrogen samples.

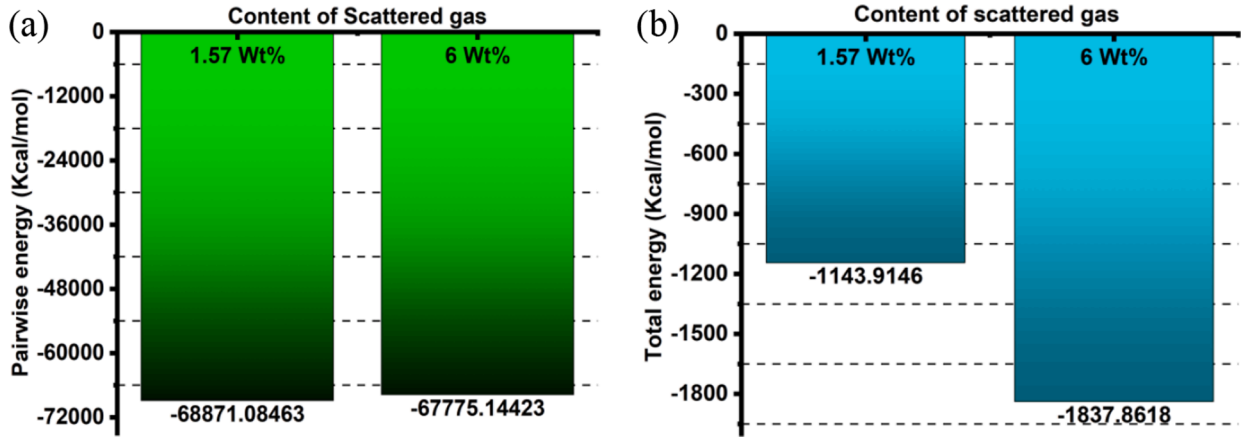

Fig. 14. The average of (a) pairwise energy of dodecane sample, and (b) the total energy between gas and host liquid in isooctane sample.

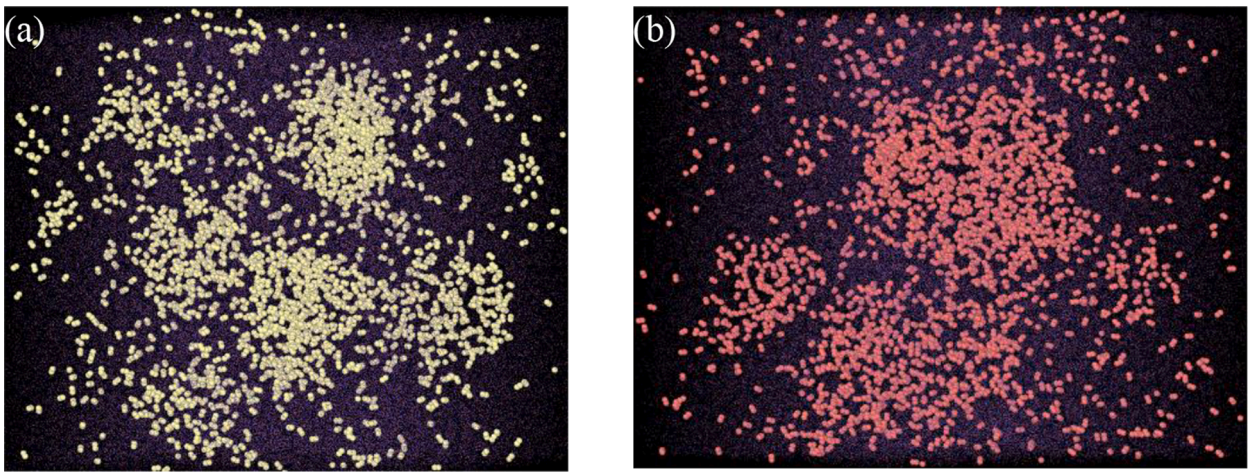

Fig. 15. Snapshots of the formed NBs in dodecane sample at (a) 298.15 K and (b) 343.15 K at 0.5 ns.

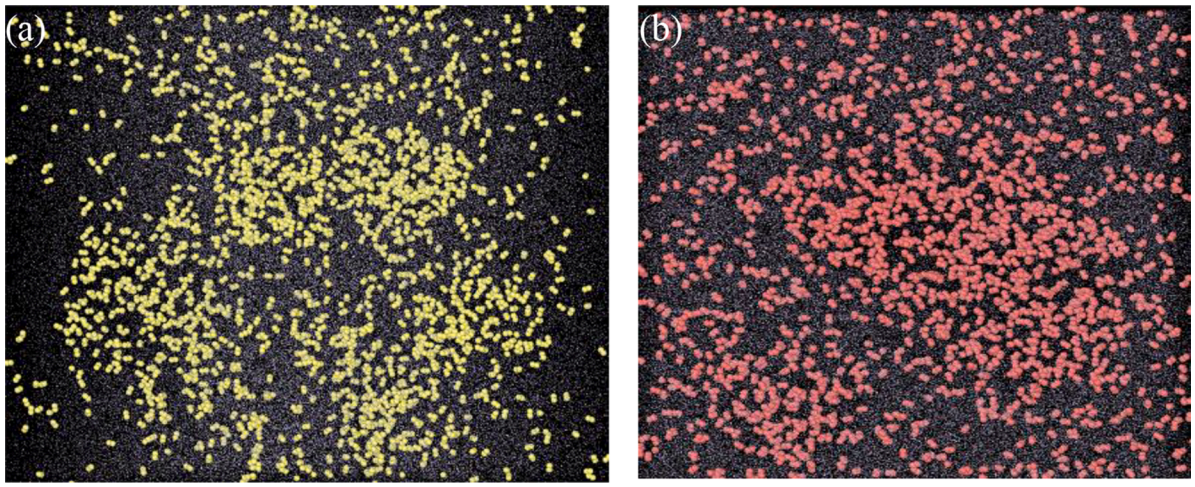

Fig. 16. Snapshots of the formed NBs in isooctane sample at (a) 298.15 K and (b) 343.15 K at 0.5 ns.

Fig. 13 compares the specific heat capacity of mixtures with different gas weight fraction. It is noted for the prepared dodecane samples with the increase in gas weight fraction, the specific heat capacity is lowered. In contrast, the prepared isooctane sample at lower gas weight fraction has much lower heat capacity compared to the base isooctane, while a higher gas weight fraction at 6 wt% slightly increases the specific heat capacity. This behavior has been observed in an experimental study in which by increasing the weight fraction of dispersed materials in dispersive medium, the heat capacity increases initially and then decreases [57]. It is proposed that there is an optimal weight fraction that a higher or lower weight fraction can lead to the reduction of the specific heat capacity [55]. Therefore, the results shown in Fig. 13 indicate that dodecane has lower optimal weight fraction than isooctane that by increasing the weight fraction of the scattered gas above 1.57 wt%, the specific heat decrease.

Fig. 14 shows the average pairwise energy of dodecane samples and

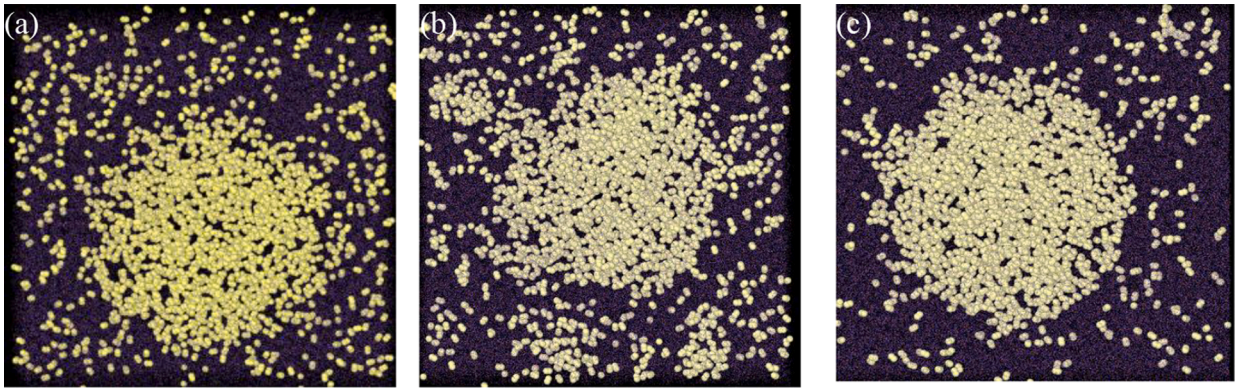

Fig. 17. Snapshots of the formed NBs (a) at higher temperature at 1.5 ns, (b) at lower temperature at 1.5 ns and (c) at 4.75 ns in dodecane.

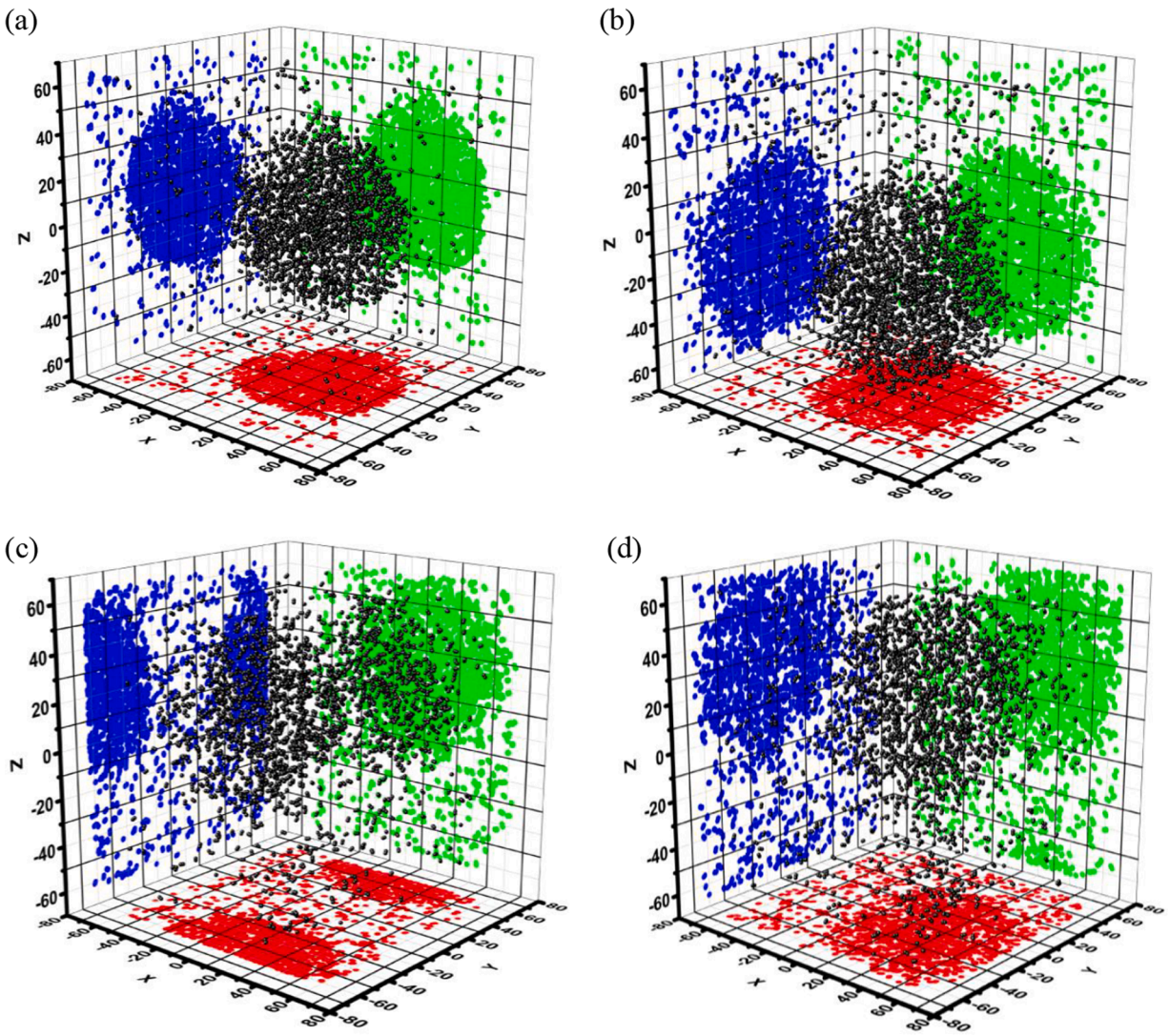

Fig. 18. Snapshots of formed NBs in (a, b) dodecane and (c, d) isooctane (a, c) at lower and (b, d) higher temperature.

total energy between gas and liquid in isooctane samples. It can be seen in Fig. 14 (a) that by increasing the weight fraction of scattered gas in the dodecane samples, pairwise energy of the system decreases and lead to the reduction in the specific heat capacity. In addition, it was suggested that three mechanisms play important roles in enhancing heat capacity of base fluids by adding additives, including the increase in surface energy, a high thermal resistance between base fluid and nanoparticles, and semi solidification of liquid layers around the dispersed nanoparticles in host liquids[57]. Scrutinizing the attractive force between nitrogen and isooctane molecules reveals that by rising the weight fraction of the dispersed gas from 1.57 to 6 wt%, the attractive force between host liquid and scattered gas atoms is increased by 60%, which leads to the increase in heat capacity of isooctane host mixture. Hu et al. [58] found that by increasing the weight fraction of scattered nanoparticles in eutectic salt-silica nanofluid for solar energy storage, the heat capacity is improved initially and then decreased. Their analysis confirmed that by increasing the weight fraction of dispersed particles, the potential energy of the system is increased to the optimum point and the further increase in the weight fraction of the addictive leads to the decrease in both potential energy and heat capacity.

3.3. Effect of temperature

Samples with the same weight fraction of the dispersed gas were studied at two different temperatures, 298.15 and 343.15 K. The number of initial clusters formed at higher temperature is less than that at the lower temperature, however the size of initial clusters at higher temperature samples is larger. Fig. 15 and Fig. 16 show the snapshots of the formed NBs in dodecane and isooctane samples at 298.15 K and 343.15 K at 0.5 ns. It is noted that three and two clusters are formed in dodecane and isooctane samples, respectively, at 343.15 K. In contrast, more small clusters have been observed at lower temperature.

Fig. 17 shows the snapshots of the formed NBs at higher temperature at 1.5 ns and lower temperature at 1.5 ns and 4.75 ns. The results indicate that the coalescence process of the formed NBs is faster at higher temperature than that at lower temperature, as the coalescence process finishes at 1.5 ns at higher temperature sample; it takes 4.75 ns to complete the coalescence at lower temperature.

Fig. 18 shows the snapshots of formed NBs in dodecane and isooctane at lower and higher temperature, and indicates that the size of the formed NBs at 13.4 ns is roughly the same for each combination. Therefore, it can be concluded that temperature doesn't have significant effect on the size of the formed NBs in a long period of time, however as it does affect the coalescence process at initial time.

In comparison to the viscosity of samples at environmental temperature (Table 3), by increasing temperature, the viscosity of the prepared samples is decreased by 21.93% and 49.65% for the prepared dodecane and isooctane samples, respectively. It follows the general trend that the

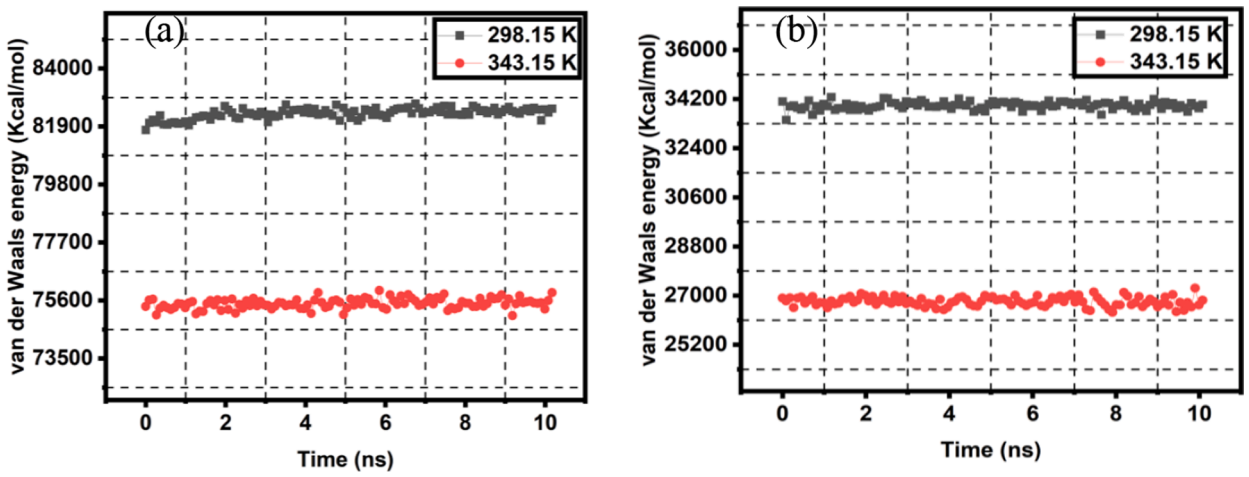

Fig. 19. Absolute amount of van der Waals energy of (a) dodecane and (b) isooctane at different temperatures.

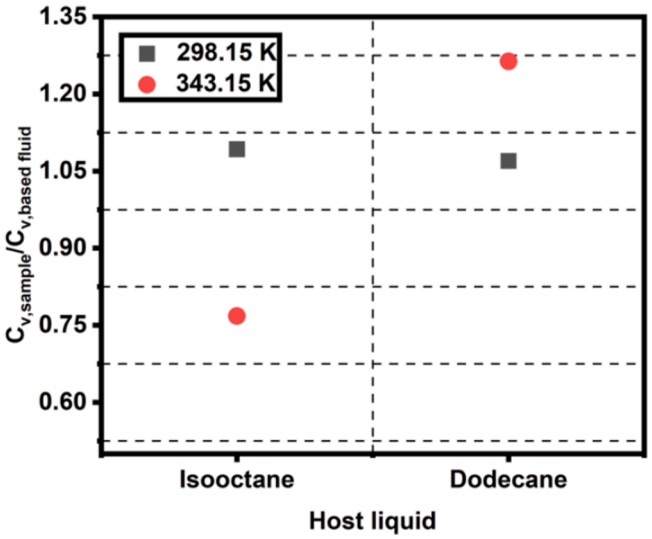

Fig. 20. The specific heat capacity of prepared samples at different temperature.

viscosity of liquids decreases with the increase of temperature [56]. However, the results reveal that the type of host liquid plays an important role in the viscosity of the prepared sample, and in this case the viscosity of isooctane sample has much higher sensitivity to the temperature change. From molecular perspective, attractive intermolecular forces between the host liquid and dispersed gas decreases with the increase in temperature. Therefore, the van der Waals interaction is reduced at higher temperature, as shown in Fig. 19, which increases the momentum transfer between the layers of molecules of the prepared samples and decreases the viscosity.

It is also observed that the diffusion coefficient of the prepared samples is increased by 102.92% and 112.43% for isooctane and dodecane samples, respectively, when the temperature is increased from 298.15 K to 343.15 K. Therefore, the molecules of the prepared samples can move more easily at higher temperature.

Understanding of the effect of temperature on thermal properties, especially the specific heat capacity, is vital as they can influence the application of materials. Generally speaking, heat capacity decreases with the increase in temperature[59]. Fig. 20 compares the specific heat capacity of prepared samples at different temperature. The specific isochoric heat capacity of isooctane sample is decreased by increasing temperature, while the specific heat capacity of dodecane sample shows an opposite trend that it increases with the increase in temperature. Similar trend has been observed by other researchers that specific heat capacity of PCM-based mixture can be increased at higher temperature [53,58,60].

Fig. 21 shows the pairwise energy of isooctane and coulomb energy of dodecane samples at 298.15 K and 343.15 K. The results indicate that in the isooctane sample, non-bonded stored energy decreases with the

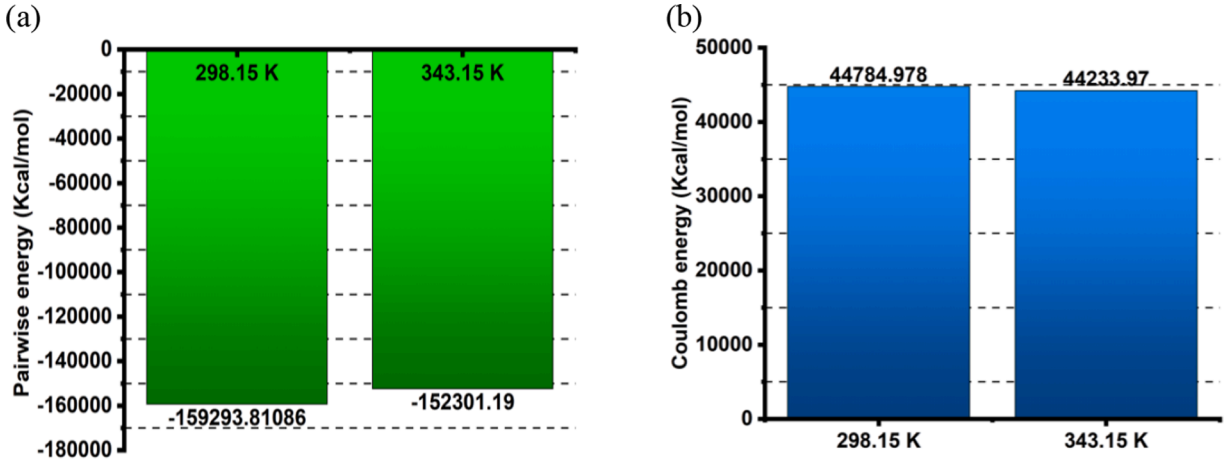

Fig. 21. (a) Pairwise energy of isooctane and (b) coulomb energy of dodecane samples at 298.15 K and 343.15 K.

increase in temperature and causes the decrease in specific heat capacity. However, rising temperature leads to a decrease in the repulsive force of the dodecane sample, intensifying the collision of molecules and increasing the energy distribution and specific heat capacity. The analysis reveals the strong dependency of the heat capacity of mixtures at higher temperature on molecular interactions of host liquid.

4. Conclusion

In this paper, the formation, coalescence and behavior of formed NBs of different gases in the phase change material dodecane and fuel host isooctane and their thermal properties were investigated by molecular dynamics simulations. The main conclusions can be drawn as follows:

(1) Formation of NBs and the speed of coalescence process are highly depended on the molecular interactions between host liquids and dispersed gases. Oxygen could form NBs in dodecane host but it could not generate any NBs in the isooctane sample. The viscosity of the prepared samples strongly depends on this interaction as adding oxygen to dodecane causes an increase in attractive forces and the viscosity. While repulsive force can be intensified by adding carbon dioxide, which decreases the viscosity.
(2) Due to the enhancement of molecular collisions by increasing the attractive forces, specific heat capacity of samples with NBs is higher than those without NBs.
(3) Nucleation of NBs strongly depends on the weight fraction of dispersed gases and by decreasing the weight fraction of dissolved gases, the probability of NBs formation decreases. In addition, by reducing the weight fraction of the scattered gas, the number of gas atoms around the host liquid atom decreases, which results in the increase in their mobility and reduces the viscosity.
(4) Specific heat capacity highly depends on the weight fraction of the scattered gas and type of host fluids. For dodecane with long chain molecules, stored energy in the system decreases with the increase of weight fraction of dispersed gas, which reduces the heat capacity of the sample. In contrast, in the isooctane sample by increasing the weight fraction of the scattered gas, attractive force increases and leads to the increase in the specific heat capacity.
(5) Increasing temperature enhances coalescence process. However, the effect of temperature on specific isochoric heat capacity highly depends on molecular interaction between the host liquid and addictive. For dodecane samples, by increasing temperature, repulsive force decreases and leads to an increase in collision of long chain molecules of dodecane, as well as the heat capacity. On the other hand, in isooctane samples, the stored energy of system is decreased by increasing temperature, which decreases specific heat capacity.

CRediT authorship contribution statement

Hamidreza Hassanloo: Writing – review & editing, Writing – original draft, Visualization, Software, Methodology, Investigation, Formal analysis, Data curation. **Xinyan Wan:** Supervision,Writing – review & editing.

Declaration of Competing Interest

The authors declare that they have no known competing financial interests or personal relationships that could have appeared to influence the work reported in this paper.

Data availability

The data of this paper can be accessed from the Brunel University London data archive, figshare at https://brunel.figshare.com

Acknowledgement

This work was supported by a UKRI Future Leaders Fellowship (MR/T042915/1) and EPSRC DTP (EP/T518116/1-2688449). MD simulations were run on ARCHER2 and MMM Hub Young, the UK's National Supercomputing Service, the data of this paper can be accessed from the Brunel University London data archive, figshare at https://brunel.figshare.com.

Appendix A. Supplementary data

Supplementary data to this article can be found online at https://doi.org/10.1016/j.fuel.2023.130254.

References

[1] Alheshibri M, Qian J, Jehannin M, Craig VS. A history of nanobubbles. Langmuir 2016;32(43):11086–100.
[2] Pérez-Lombard L, Ortiz J, Pout C. A review on buildings energy consumption information. Energ Buildings 2008;40(3):394–8.
[3] Nkwetta DN, Haghighat F. Thermal energy storage with phase change material—A state-of-the art review. Sustain Cities Soc 2014;10:87–100.
[4] Nazir H, et al. Recent developments in phase change materials for energy storage applications: A review. Int J Heat Mass Transf 2019;129:491–523.
[5] Oh SH, Yoon SH, Song H, Han JG, Kim J-M. Effect of hydrogen nanobubble addition on combustion characteristics of gasoline engine. Int J Hydrogen Energy 2013;38(34):14849–53.
[6] Agarwal A, Ng WJ, Liu Y. Principle and applications of microbubble and nanobubble technology for water treatment. Chemosphere 2011;84(9):1175–80.
[7] Temesgen T, Bui TT, Han M, Kim T-I, Park H. Micro and nanobubble technologies as a new horizon for water-treatment techniques: A review. Adv Colloid Interface Sci 2017;246:40–51.
[8] Epstein PS, Plesset MS. On the stability of gas bubbles in liquid-gas solutions. J Chem Phys 1950;18(11):1505–9.
[9] Nirmalkar N, Pacek A, Barigou M. On the existence and stability of bulk nanobubbles. Langmuir 2018;34(37):10964–73.
[10] Sajid MU, Ali HM. Thermal conductivity of hybrid nanofluids: a critical review. Int J Heat Mass Transf 2018;126:211–34.
[11] Bayda S, Adeel M, Tuccinardi T, Cordani M, Rizzolio F. The history of nanoscience and nanotechnology: from chemical–physical applications to nanomedicine. Molecules 2019;25(1):112.
[12] Lagache M, Ungerer P, Boutin A, Fuchs A. Prediction of thermodynamic derivative properties of fluids by Monte Carlo simulation. PCCP 2001;3(19):4333–9.
[13] Riniker S, Allison JR, van Gunsteren WF. On developing coarse-grained models for biomolecular simulation: a review. PCCP 2012;14(36):12423–30.
[14] Jabbari F, Rajabpour A, Saedodin S. Thermal conductivity and viscosity of nanofluids: A review of recent molecular dynamics studies. Chem Eng Sci 2017;174:67–81.
[15] Hassanloo H, Sadeghzadeh S, Ahmadi R. Reactive molecular dynamics simulation of thermo-physicochemical properties of non-covalent functionalized graphene nanofluids. Mater Today Commun 2022;32:103869.
[16] Satoh A. Introduction to practice of molecular simulation: molecular dynamics, Monte Carlo, Brownian dynamics, Lattice Boltzmann and dissipative particle dynamics. Elsevier; 2010.
[17] Sinha-Ray S, Sinha-Ray S, Sriram H, Yarin AL. Flow of suspensions of carbon nanotubes carrying phase change materials through microchannels and heat transfer enhancement. Lab Chip 2014;14(3):494–508.
[18] Phan K, Truong T, Wang Y, Bhandari B. Effect of CO2 nanobubbles incorporation on the viscosity reduction of fruit juice concentrate and vegetable oil. Int J Food Sci Technol 2021;56(9):4278–86.
[19] Lu Y. Drag reduction by nanobubble clusters as affected by surface wettability and flow velocity: Molecular dynamics simulation. Tribol Int 2019;137:267–73.
[20] Maheshwari S, van der Hoef M, Prosperetti A, Lohse D. Dynamics of formation of a vapor nanobubble around a heated nanoparticle. J Phys Chem C 2018;122(36):20571–80.
[21] Wang Y, Chen Z, Ling X. A molecular dynamics study of nano-encapsulated phase change material slurry. Appl Therm Eng 2016;98:835–40.
[22] Chatzis G, Samios J. Binary mixtures of supercritical carbon dioxide with methanol. A molecular dynamics simulation study. Chem Phys Lett 2003;374(1–2):187–93.
[23] Zhao X, Jin H, Chen Y, Ge Z. Numerical study of H2, CH4, CO, O2 and CO2 diffusion in water near the critical point with molecular dynamics simulation. Comput Math Appl 2021;81:759–71.
[24] Xu W, et al. The generation and stability of bulk nanobubbles by compression-decompression method: The role of dissolved gas. Colloids Surf A Physicochem Eng Asp 2023;657:130488.
[25] Lee JI, Yim B-S, Kim J-M. Effect of dissolved-gas concentration on bulk nanobubbles generation using ultrasonication. Sci Rep 2020;10(1):18816.

[26] Li Q, Ying Y-L, Liu S-C, Hu Y-X, Long Y-T. Measuring temperature effects on nanobubble nucleation via a solid-state nanopore. Analyst 2020;145(7):2510–4.
[27] Jabbarzadeh A, Harrowell P, Tanner R. The structural origin of the complex rheology in thin dodecane films: Three routes to low friction. Tribol Int 2007;40 (10–12):1574–86.
[28] Zhao L, et al. Combined experimental and computational study on the unimolecular decomposition of JP-8 jet fuel surrogates. I. n-Decane (n-C10H22). Chem A Eur J 2017;121(6):1261–80.
[29] Song Y, Zhang N, Jing Y, Cao X, Yuan Y, Haghighat F. Experimental and numerical investigation on dodecane/expanded graphite shape-stabilized phase change material for cold energy storage. Energy 2019;189:116175.
[30] Darvin JR, Hossain MS, Nabil M, Uertz J, Mills G. Concentrated Ag nanoparticles in dodecane as phase change materials for thermal energy storage. ACS Appl Nano Mater 2019;2(10):6187–96.
[31] Ershov M, Potanin D, Tarazanov S, Abdellatief TM, Kapustin V. Blending characteristics of isooctene, MTBE, and TAME as gasoline components. Energy Fuel 2020;34(3):2816–23.
[32] Schmitt S, et al. Effects of water addition on the combustion of iso-octane investigated in laminar flames, low-temperature reactors, and an HCCI engine. Combust Flame 2020;212:433–47.
[33] Kritikos E, Giusti A. Investigation of the effect of iron nanoparticles on n-dodecane combustion under external electrostatic fields. In: Proceedings of the Combustion Institute; 2022.
[34] Gobinath S, Senthilkumar G, Beemkumar N. Air nanobubble-enhanced combustion study using mustard biodiesel in a common rail direct injection engine. Energy Sources Part A 2019;41(15):1809–16.
[35] Amburi PK, Senthilkumar G, Neme Mogose I. Heat Transfer Augmentation: Experimental Study with Nanobubbles Technology. Adv Mater Sci Eng 2022;vol: 2022.
[36] Bader R. Quantum topology of molecular charge distributions. III. The mechanics of an atom in a molecule. J Chem Phys 1980;73(6):2871–83.
[37] Tannor DJ, et al. Accurate first principles calculation of molecular charge distributions and solvation energies from ab initio quantum mechanics and continuum dielectric theory. J Am Chem Soc 1994;116(26):11875–82.
[38] Varga K, Driscoll JA. Computational nanoscience: Applications for molecules, clusters, and solids. Cambridge University Press; 2011.
[39] Balyakin I, Yuryev A, Gelchinski B, Rempel A. Ab initio molecular dynamics and high-dimensional neural network potential study of VZrNbHfTa melt. J Phys Condens Matter 2020;32(21):214006.
[40] Hoover WG, Evans DJ, Hickman RB, Ladd AJ, Ashurst WT, Moran B. Lennard-Jones triple-point bulk and shear viscosities. Green-Kubo theory, Hamiltonian mechanics, and nonequilibrium molecular dynamics. Phys Rev A 1980;22(4):1690.
[41] Allen MP. Introduction to molecular dynamics simulation. Computational soft matter: from synthetic polymers to proteins 2004;23(1):1–28.
[42] Sun H. COMPASS: an ab initio force-field optimized for condensed-phase applications overview with details on alkane and benzene compounds. J Phys Chem B 1998;102(38):7338–64.
[43] Yang Q, Zhong C. Molecular simulation of adsorption and diffusion of hydrogen in metal– organic frameworks. J Phys Chem B 2005;109(24):11862–4.
[44] Chae K, Violi A. Mutual diffusion coefficients of heptane isomers in nitrogen: A molecular dynamics study. J Chem Phys 2011;134(4):044537.
[45] Sun C, Wen B, Bai B. Application of nanoporous graphene membranes in natural gas processing: Molecular simulations of CH4/CO2, CH4/H2S and CH4/N2 separation. Chem Eng Sci 2015;138:616–21.
[46] Jain S, Qiao L. Molecular dynamics simulations of the surface tension of oxygen-supersaturated water. AIP Adv 2017;7(4):045001.
[47] Plimpton S. Fast parallel algorithms for short-range molecular dynamics. J Comput Phys 1995;117(1):1–19.
[48] Stukowski A. Visualization and analysis of atomistic simulation data with OVITO–the Open Visualization Tool. Model Simul Mater Sci Eng 2009;18(1): 015012.
[49] Pádua A, Fareleira J, Calado J, Wakeham W. Density and viscosity measurements of 2, 2, 4-trimethylpentane (isooctane) from 198 K to 348 K and up to 100 MPa. J Chem Eng Data 1996;41(6):1488–94.
[50] Tofts PS, et al. Test liquids for quantitative MRI measurements of self-diffusion coefficient in vivo. Magnetic Resonance in Medicine: An Official Journal of the International Society for Magnetic Resonance in Medicine 2000;43(3):368–74.
[51] Caudwell D, Trusler J, Vesovic V, Wakeham W. The viscosity and density of n-dodecane and n-octadecane at pressures up to 200 MPa and temperatures up to 473 K. Int J Thermophys 2004;25(5):1339–52.
[52] Ohgaki K, Khanh NQ, Joden Y, Tsuji A, Nakagawa T. Physicochemical approach to nanobubble solutions. Chem Eng Sci 2010;65(3):1296–300.
[53] Tafrishi H, Sadeghzadeh S, Ahmadi R, Molaei F, Yousefi F, Hassanloo H. Investigation of tetracosane thermal transport in presence of graphene and carbon nanotube fillers—A molecular dynamics study. J Storage Mater 2020;29:101321.
[54] Yu Y, Zhao C, Tao Y, Chen X, He Y-L. Superior thermal energy storage performance of NaCl-SWCNT composite phase change materials: A molecular dynamics approach. Appl Energy 2021;290:116799.
[55] Hansen J-P, McDonald IR. Theory of simple liquids.
[56] Dembicki H. Practical petroleum geochemistry for exploration and production. Elsevier; 2022.
[57] Ho MX, Pan C. Optimal concentration of alumina nanoparticles in molten Hitec salt to maximize its specific heat capacity. Int J Heat Mass Transf 2014;70:174–84.
[58] Hu Y, He Y, Zhang Z, Wen D. Enhanced heat capacity of binary nitrate eutectic salt-silica nanofluid for solar energy storage. Sol Energy Mater Sol Cells 2019;192: 94–102.
[59] Engelmann S, Hentschke R. Specific heat capacity enhancement studied in silica doped potassium nitrate via molecular dynamics simulation. Sci Rep 2019;9(1): 1–14.
[60] Rao Z, Wang S, Peng F. Molecular dynamics simulations of nano-encapsulated and nanoparticle-enhanced thermal energy storage phase change materials. Int J Heat Mass Transf 2013;66:575–84.